



Cite this: *Chem. Sci.*, 2023, **14**, 4923

All publication charges for this article have been paid for by the Royal Society of Chemistry

Received 13th March 2023  
 Accepted 4th April 2023

DOI: 10.1039/d3sc01347b  
[rsc.li/chemical-science](http://rsc.li/chemical-science)

## Introduction

The established benefit of fluorine-containing fragments in medicinal chemistry relies on their ability to alter the physicochemical and pharmacokinetic properties of organic compounds.<sup>1</sup> In addition, it is acknowledged that increasing  $C(sp^3)$  incorporation and the presence of stereogenic centres positively correlate with the clinical success of small molecule therapeutics.<sup>2</sup> These aspects explain the importance of developing novel methods for the stereoselective incorporation of trifluoromethyl ( $CF_3$ ) and perfluoroalkyl ( $R_F$ ) units within organic molecules. However, only a few strategies are available for the catalytic production of perfluoroalkyl-containing stereogenicity.<sup>3</sup> For example, the combination of enamine organocatalysis and photoredox catalysis served to develop the enantioselective  $\alpha$ -perfluoroalkylation of aldehydes (Fig. 1a).<sup>4</sup> In a different photochemical approach, the asymmetric  $\alpha$ -perfluoroalkylation of  $\beta$ -ketoesters was reported under phase transfer catalysis (PTC, Fig. 1b).<sup>5</sup> Both protocols used visible light to generate perfluoroalkyl radicals ( $R_F^\bullet$ , **I**) via single electron transfer (SET), which were then intercepted stereoselectively. The photochemical radical generation was mastered either by an external photocatalyst (Fig. 1a) or by excitation of a ground-state electron donor–acceptor (EDA) complex<sup>6</sup>

## Enantioselective catalytic remote perfluoroalkylation of $\alpha$ -branched enals driven by light<sup>†‡</sup>

Matteo Balletti,<sup>a</sup> Tommy Wachsmuth,<sup>id</sup> <sup>a</sup> Antonio Di Sabato,<sup>id</sup> <sup>a</sup> Will C. Hartley<sup>a</sup> and Paolo Melchiorre<sup>id</sup> <sup>a,b</sup>

Herein, we report a photochemical organocatalytic method for the asymmetric introduction of perfluoroalkyl fragments (including the valuable trifluoromethyl moiety) at the remote  $\gamma$ -position of  $\alpha$ -branched enals. The chemistry exploits the ability of extended enamines (dienamines) to form photoactive electron donor–acceptor (EDA) complexes with perfluoroalkyl iodides, which under blue light irradiation generate radicals through an electron transfer mechanism. The use of a chiral organocatalyst, derived from *cis*-4-hydroxy-L-proline, secures a consistently high stereocontrol while inferring complete site selectivity for the more distal  $\gamma$  position of the dienamines.

between perfluoroalkyl iodides and a chiral enolate (Fig. 1b). These methods led to the formation of  $C(sp^3)-CF_3$  and  $C(sp^3)-R_F$  stereocenters at the  $\alpha$  position of carbonyl compounds. In

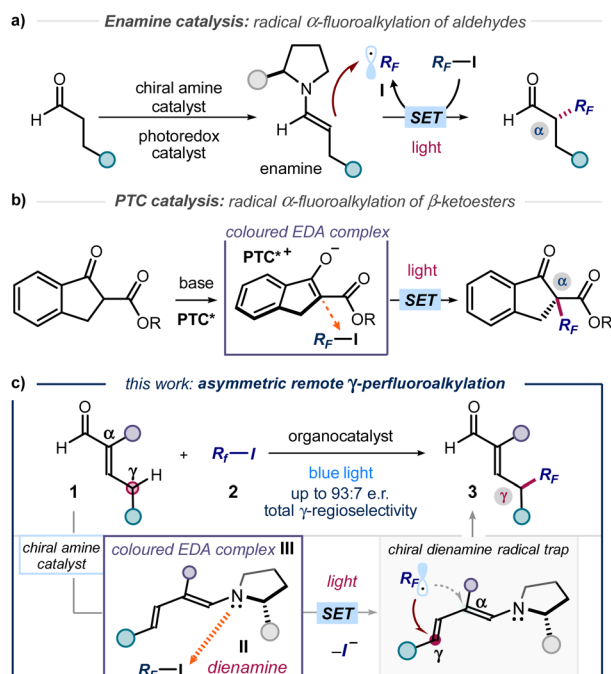


Fig. 1 Organocatalytic photochemical strategies for the stereo-selective radical  $\alpha$ -perfluoroalkylation of (a) aldehydes and (b)  $\beta$ -ketoesters. (c) Design plan for the stereocontrolled radical perfluoroalkylation of enals at the remote  $\gamma$ -carbon via excitation of an EDA complex III between a catalytic dienamine II and perfluoroalkyl iodides. PTC: phase transfer catalyst; EDA: electron donor–acceptor;  $R_F$ : perfluoroalkyl chain.

<sup>a</sup>ICIQ – Institute of Chemical Research of Catalonia, 43007 Tarragona, Spain

<sup>b</sup>Department of Industrial Chemistry 'Toso Montanari', University of Bologna, 40136 Bologna, Italy. E-mail: [p.melchiorre@unibo.it](mailto:p.melchiorre@unibo.it)

† Dedicated to the 70th birthday of Professor Dennis Curran.

‡ Electronic supplementary information (ESI) available: details of experimental procedures, full characterization data, and copies of NMR spectra (PDF). Crystallographic data for compound 3g has been deposited with the Cambridge Crystallographic Data Centre. CCDC 2215186. For ESI and crystallographic data in CIF or other electronic format see DOI: <https://doi.org/10.1039/d3sc01347b>



contrast, strategies that account for the stereoselective installation of perfluoroalkyl units at distal positions of the substrates are not available. Herein, we close this gap in synthetic methodology by disclosing a photochemical method for the asymmetric introduction of  $\text{CF}_3$  and  $\text{R}_\text{F}$  groups at the remote  $\gamma$  position of  $\alpha$ -branched enals **1** (Fig. 1c).

## Design plan

Our plan for the remote perfluoroalkylation relied on the reactivity of chiral dienamines **II**, generated upon activation of  $\alpha$ -branched enals **1** with a chiral amine catalyst (Fig. 1c). Intermediates **II** are characterized by vinylogous nucleophilicity,<sup>7</sup> and have been used for the site-selective functionalization of enals **1** at their remote  $\gamma$ -carbon *via* traditional two-electron ionic pathways.<sup>8</sup> Recently, we demonstrated that the dienamine activation platform could be translated successfully also to radical chemistry.<sup>9</sup> The use of an external catalyst secured formation of electrophilic radicals, which were then stereoselectively intercepted by the chiral dienamine at remote position.<sup>9a</sup> In the context of  $\text{C}(\text{sp}^3)\text{-R}_\text{F}$  bond formation, we surmised that the electron-rich nature of **II** could be leveraged to form photoactive EDA complexes upon aggregation with perfluoroalkyl iodides.<sup>5,10</sup> Visible light excitation of the EDA complex **III** would then drive the formation of perfluoroalkyl radical ( $\text{R}_\text{F}^\bullet$ , **I**), thus circumventing the need of an exogenous photocatalyst. Regio- and stereoselective trap would then offer a catalytic strategy for the remote  $\gamma$ -perfluoroalkylation of  $\alpha$ -branched enals **1**.

## Results and discussion

The feasibility of our plan was evaluated by reacting 2-phenyl pentenal **1a** with nonafluoroiodobutane **2a** in  $\text{Et}_2\text{O}$  using the commercially available TMS-protected diphenyl prolinol catalyst **A** (20 mol%, TMS: trimethylsilyl) and 2,6-lutidine as the additive (Fig. 2a). We noticed that the reaction mixture turned immediately yellow right after addition of all the reaction components, which individually were colorless (see below for further details). Irradiation by a blue light LED afforded the desired product (*R*)-**3a** with complete  $\gamma$ -regioselectivity and good enantiomeric ratio, albeit in low yield (37% yield, 82 : 18 e. r.). Other solvents, including THF and dichloromethane, were suitable, but diethyl ether proved optimal (see Section E of the ESI‡ for full optimization studies).

To improve the stereoselectivity of the remote perfluoroalkylation, we modified the catalyst structure. Introduction of fluorinated aryl motifs (3,5-difluorophenyl and 3,5-bis(trifluoromethyl) substituents) in catalysts **B** and **C** improved the yield significantly, but the enantioselectivity remained unsatisfactory. Structural variation of the best-performing catalyst **C** focused on the effect of different silyl ether substituents (catalysts **C**–**G**). These studies, detailed in Fig. 2b, revealed that the smallest TMS group in catalyst **C** outperformed larger silyl ethers in terms of yield and enantioselectivity (93%, 84 : 16 e. r.). We next investigated the effect of a second stereogenic element on the catalyst's pyrrolidine core by synthesizing

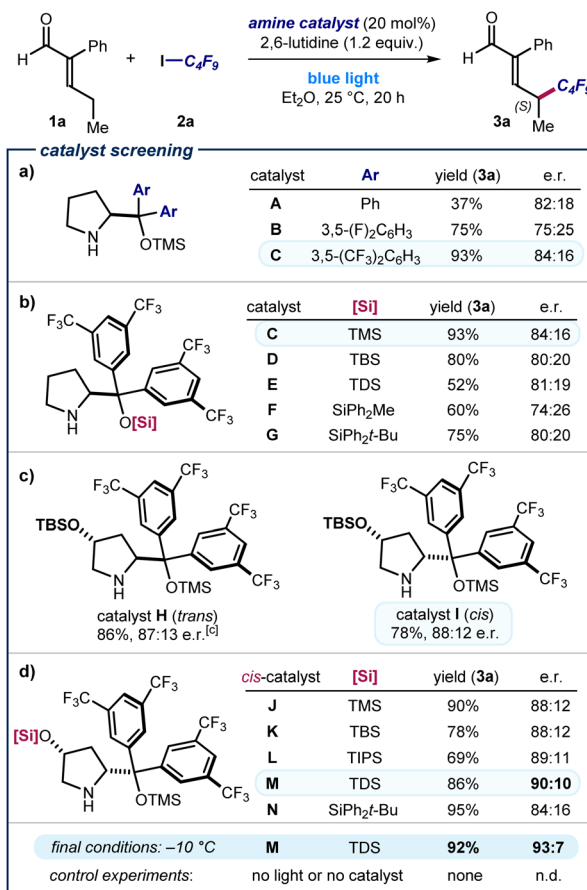


Fig. 2 (a–d) Catalyst optimization. Reactions performed for 20 h in 0.3 mL of  $\text{Et}_2\text{O}$  using 0.2 mmol of **2a**, 0.6 mmol of **1a**, and 0.04 mmol of catalyst (20 mol%) under irradiation by a single high-power LED ( $\lambda_{\text{max}} = 460\text{ nm}$ , irradiance =  $100\text{ mW cm}^{-2}$ ). Yield of **3a** determined by  $^1\text{H}$  NMR analysis of the crude mixture using trimethyl orthoformate as the internal standard. Enantiomeric ratio (e. r.) of **3a** measured by chiral UPC<sup>2</sup> analysis after derivatization to the corresponding 2,4-dinitrophenyl hydrazone. Note that catalysts **A**–**H** gave product **3a** with an (*R*) absolute configuration; the figure shows the (*S*) major enantiomer of **3a** afforded by catalysts **I**–**M**. TMS: trimethylsilyl; TBS: *tert*-butyldimethylsilyl; TIPS: triisopropylsilyl; TDS: thexyldimethylsilyl.

variants derived from 4-hydroxyproline (Fig. 2c).<sup>11</sup> The *tert*-butyldimethylsilyl (TBS)-protected catalyst **H**, derived from *trans*-4-hydroxyproline, offered an increased stereocontrol (87 : 13 e. r.). The diastereomeric catalyst **I**, bearing the two pyrrolidine ring substituents in a *cis* relationship,<sup>12</sup> led to a slightly increased stereocontrol (the opposite enantiomer of the product (*S*)-**3a** was formed in 88 : 12 e. r.). This result suggested us to further optimize the structure of catalysts derived from *cis*-4-hydroxyproline (Fig. 2d). Assessment of different silyl ether protecting groups at the 4-hydroxy moiety identified the bulky thexyldimethylsilyl (TDS)-protected catalyst **M** as the best-performing, since product **3a** was obtained in 90 : 10 e. r. Lowering the reaction temperature to  $-10^\circ\text{C}$  afforded **3a** in 93 : 7 e. r. and in excellent yield. Control experiments established that both the amine catalyst and light were essential for reactivity.



To evaluate the generality of the method, we applied the optimized conditions and the *cis*-catalyst **M** to react enal **1a** with iodides of different perfluoroalkyl chain lengths (Fig. 3a). Pleasingly, products **3a–g** were obtained in good to high yields and enantiomeric ratios. Only reaction at the remote position occurred, exclusively leading to  $\gamma$ -functionalized products.

Crystals of compound **3g** were suitable for X-ray crystallographic analysis, which allowed the (*S*) configuration of the newly formed stereocenter to be assigned unambiguously. Ethyl difluoroiodoacetate could be used as the radical precursor, enabling the synthesis of  $\alpha$ -difluoro ester **3h** in good yield and enantioselectivity. A sensitive sulfonyl fluoride was tolerated well, affording the heteroatom-dense product **3i**. Importantly, the asymmetric formation of a  $C(sp^3)$ - $CF_3$  stereogenic center at the remote position of different enals was accomplished using  $CF_3$ -I (products **3j–l**). Other radical precursors, including perfluoroalkyl bromides and simple alkyl iodides, were unsuccessful, highlighting the need of both a weak carbon–iodine

bond and adjacent fluorine atoms (see Section C of the ESI<sup>†</sup> for a list of unsuccessful substrates).

Next, a range of substituted and functionalized enals **1** was tested (Fig. 4). Extended alkyl chain products were obtained in good yield and enantioselectivity (**3m** & **3n**), with terminal halide (adduct **3o**), ester (**3p**), benzyl (**3q**) and phenyl (**3r**) groups were well tolerated. Various substituents on the  $\alpha$ -phenyl group of enals were accepted, with products bearing alkyl (**3s** & **3t**), 4-halogen (**3u** & **3v**), and 4-methoxy (**3w**) groups all synthesized with consistently good results. In contrast, electron-withdrawing substituents (e.g., *p*-NO<sub>2</sub> and *p*-CF<sub>3</sub>) completely inhibited the reactivity. With  $\alpha$ -unsubstituted enals, achieving stereocontrol proved difficult, and the corresponding products **3x–z** were formed essentially in racemic form but with complete remote regioselectivity. A selective  $\gamma$ -perfluoroalkylation took place also with an enal derived from the naturally-occurring diterpene phytol (product **3z**). With respect to the enals

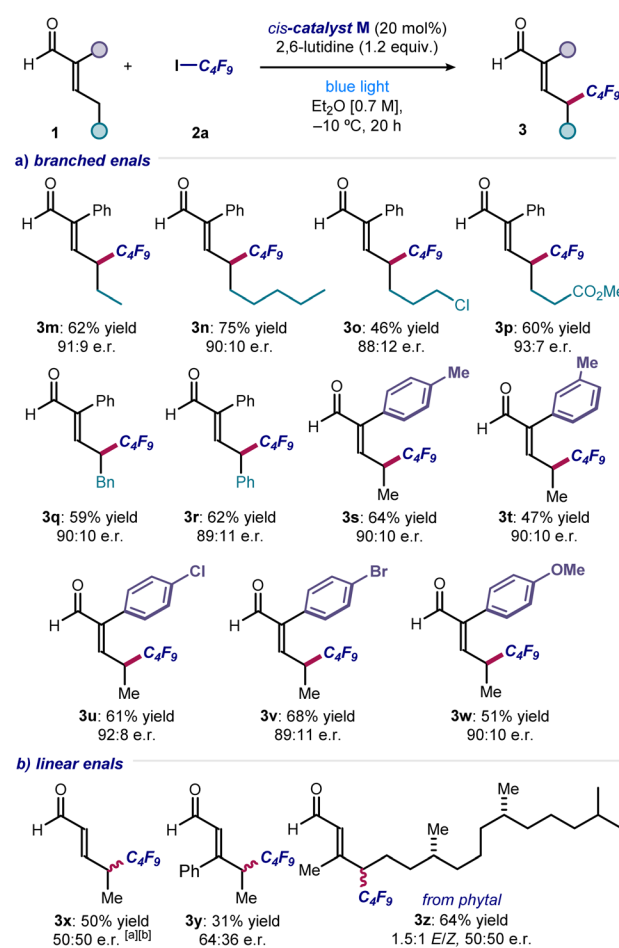
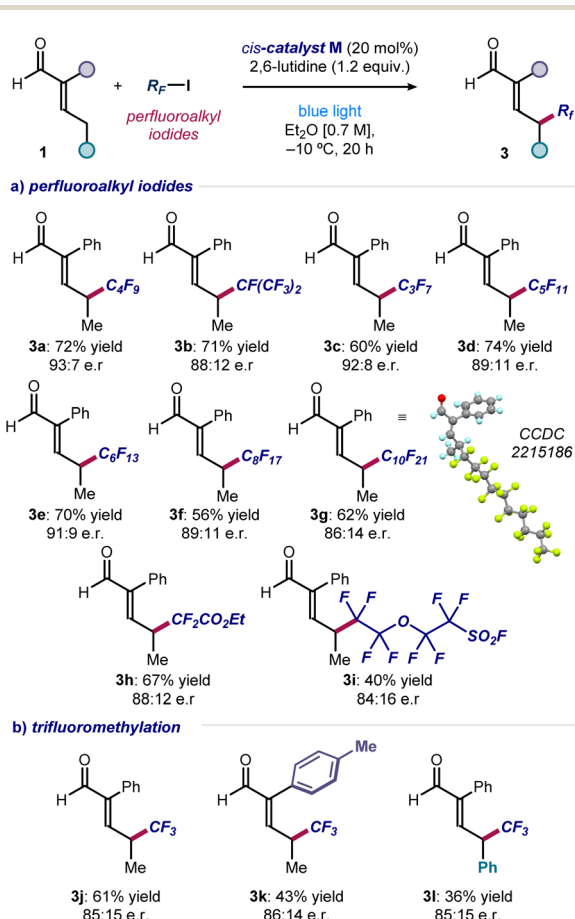


**Fig. 4 (a and b)** Different enals that can participate in the light-driven remote perfluoroalkylation. Reactions performed using **2** (0.2 mmol), enals **1** (0.6 mmol), 2,6-lutidine (0.24 mmol) in 0.3 mL of  $Et_2O$  under illumination by a single high-power LED ( $\lambda_{max} = 460$  nm, irradiance = 100 mW  $cm^{-2}$ ). Yields refer to the isolated products **3**. Enantiomeric ratios measured by  $UPC^2$  analysis on chiral stationary phase after derivatization of **3** to the corresponding 2,4-dinitrophenyl hydrazone derivatives. <sup>a</sup> Carried out at room temperature. <sup>b</sup> Isolated as the corresponding 2,4-dinitrophenyl hydrazone.

amenable to this transformation, an aryl group is required at the  $\alpha$ -position to gain high enantiocontrol, which ensures consistent configurational control over the dienamine intermediate. Enals bearing  $\alpha$ -alkyl substituents are unsuitable substrates, which undergo reaction to produce a complex mixture of side-products.

We then performed investigations to glean insight on the reaction mechanism (Fig. 5). UV-vis spectroscopic analysis confirmed that the individual components of the process were colorless, including the dienamine intermediate generated upon *in situ* from enal **1a** and the amine catalyst (green line in Fig. 5a). Right upon mixing perfluoroalkyl iodide **2a**, amino-catalyst, and enal **1a**, a new absorption band was observed in the visible region, which was further corroborated by the

appearance of a distinct yellow color of the reaction mixture. These observations are consonant with the formation of a visible-light absorbing EDA complex between the dienamine and  $R_F$ .<sup>13</sup> Mechanistically, we propose that light irradiation of the EDA complex **III** triggers an intracomplex SET, leading to the formation of perfluoroalkyl radical **I** after mesolysis of the C–I bond (Fig. 5b). The electrophilic  $R_F$ •**I** is then intercepted by the chiral dienamine **II**, in a regio- and stereoselective fashion.<sup>14</sup> The resulting  $\alpha$ -amino radical **IV** would then either deliver an electron to **2** *via* SET,<sup>15</sup> or abstract an iodine atom from **2** *via* ATRA (atom-transfer radical addition),<sup>16</sup> to regenerate the perfluoroalkyl radical **I** thus propagating the radical chain. Hydrolysis of the iminium ion intermediate **V** releases product **3** and regenerates the organocatalyst. We measured an overall quantum yield for the reaction between enal **1a** and non-afluoroiodobutane **2a** of  $\Phi = 1.14$ , which is congruent with a radical chain process being operational.<sup>17</sup>

## Conclusions

In summary, we have developed the first enantioselective methodology that accounts for the remote installation of perfluoroalkyl-containing stereogenicity. The chemistry exploits the ability of chiral catalytic dienamines to form photoactive electron donor–acceptor (EDA) complexes with perfluoroalkyl iodides, which under blue irradiation generate radicals through a SET mechanism. Key to achieving high levels of enantiocontrol and complete site selectivity for the more distal  $\gamma$  position of enals was the use of a sterically encumbered *cis*-4-hydroxyprolinol-derived catalyst.

## Data availability

Crystallographic data for compound **3g** has been deposited as CCDC 2215186. Additional experimental details and data are provided in the ESI,<sup>‡</sup> including experimental procedures, full characterization data, and copies of NMR spectra (PDF).

## Author contributions

M. B., T. W., A. S and W. C. H. performed the experiments. M. B. and P. M. conceptualized the project. P. M. directed the project. P. M. and W. C. H. wrote the manuscript with assistance from all authors.

## Conflicts of interest

There are no conflicts to declare.

## Acknowledgements

Financial support was provided by Agencia Estatal de Investigación (PID2019-106278GB-I00 and CTQ2016-75520-P). W. C. Hartley thanks the EU for a Horizon 2020 Marie Skłodowska-Curie Fellowship (H2020-MSCA-IF-2020, 101031533).

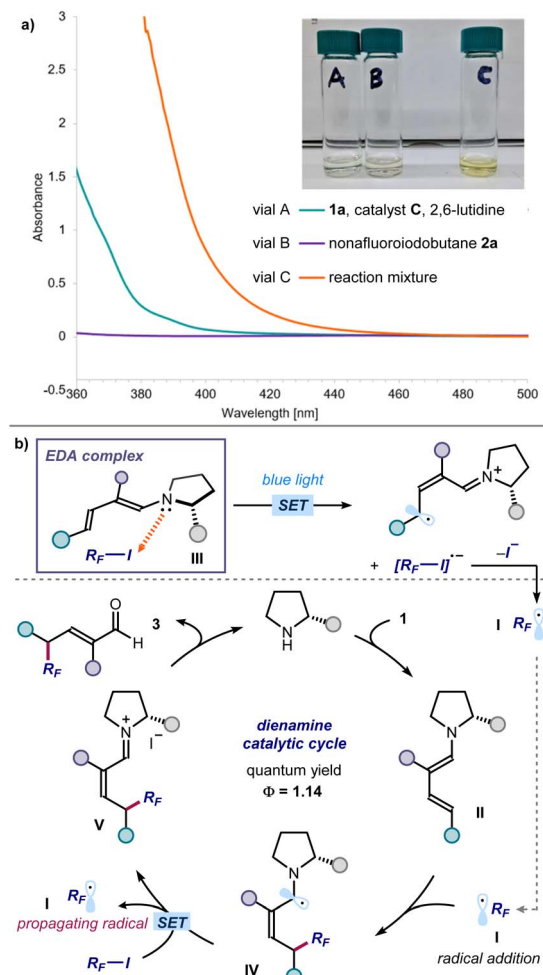


Fig. 5 Mechanistic studies. (a) UV-vis measurements acquired on a Shimadzu UV-2401PC spectrophotometer with a quartz cuvette with path length of 1 cm. All samples in Et<sub>2</sub>O. Vial A (green line): [catalyst C] = 0.6 M, [1a] = 0.6 M and [2,6-lutidine] = 0.6 M; vial B (purple line): [2a] = 0.6 M; vial C: [catalyst C] = 0.6 M, [1a] = 0.6 M, [2a] = 0.6 M and [2,6-lutidine] = 0.6 M. While the individual reaction components are all colourless, the vial C mixture containing all reaction components displays a yellow colour and an absorption band from approximately 450 nm. (b) Proposed radical propagation mechanism triggered by the excitation of the dienamine-based EDA complex **III**, which serves as the initiation event.



## References

1 (a) K. Müller, C. Faeh and F. Diederich, *Science*, 2007, **317**, 1881–1886; (b) W. K. Hagmann, *J. Med. Chem.*, 2008, **51**, 4359–4369; (c) S. Purser, P. R. Moore, S. Swallow and V. Gouverneur, *Chem. Soc. Rev.*, 2008, **37**, 320–330; (d) N. A. Meanwell, *J. Med. Chem.*, 2018, **61**, 5822–5880.

2 (a) F. Lovering, J. Bikker and J. Humblet, *J. Med. Chem.*, 2009, **52**, 6752–6756; (b) F. Lovering, *MedChemComm*, 2013, **4**, 515–519.

3 (a) A. E. Allen and D. W. C. MacMillan, *J. Am. Chem. Soc.*, 2010, **132**, 4986–4987; (b) Q.-H. Deng, H. Wadeppohl and L. H. Gade, *J. Am. Chem. Soc.*, 2012, **134**, 10769–10772; (c) H. Huo, X. Huang, X. Shen, K. Harms and E. Meggers, *Synlett*, 2015, **27**, 749–753; (d) J. Liu, W. Ding, Q.-Q. Zhou, D. Liu, L.-Q. Lu and W.-J. Xiao, *Org. Lett.*, 2018, **20**, 461–464; (e) C. Jiang, L. Wang, H. Zhang, P. Chen, Y.-L. Guo and G. Liu, *Chem.*, 2020, **6**, 2407–2419; (f) P. Xu, W. Fan, P. Chen and G. Liu, *J. Am. Chem. Soc.*, 2022, **144**, 13468–13474.

4 D. A. Nagib, M. E. Scott and D. W. C. MacMillan, *J. Am. Chem. Soc.*, 2009, **131**, 10875–10877.

5 L. Woźniak, J. J. Murphy and P. Melchiorre, *J. Am. Chem. Soc.*, 2015, **137**, 5678–5681.

6 G. E. M. Criszena, D. Mazzarella and P. Melchiorre, *J. Am. Chem. Soc.*, 2020, **142**, 5461–5476.

7 For reviews on aminocatalytic remote functionalisation strategies, see: (a) J. J. Hao, L. Albrecht and K. A. Jørgensen, *Chem. Sci.*, 2013, **4**, 2287–2300; (b) I. Jurberg, I. Chatterjee and P. Melchiorre, *Chem. Commun.*, 2013, **49**, 4869–4883. For a review on dienamine catalysis; (c) V. Marcos and J. Aleman, *Chem. Soc. Rev.*, 2016, **45**, 6812–6832. For pioneering studies on dienamine catalysis, see: (d) A. G. Nigmatov and E. P. Serebryakov, *Russ. Chem. Bull.*, 1993, **42**, 213; (e) S. Bertelsen, M. Marigo, S. Brandes, P. Diner and K. A. Jørgensen, *J. Am. Chem. Soc.*, 2006, **128**, 12973–12980.

8 For selected examples: (a) K. Liu, A. Chougnet and W. Woggon, *Angew. Chem., Int. Ed.*, 2008, **47**, 5827–5829; (b) G. Bergonzini, S. Vera and P. Melchiorre, *Angew. Chem., Int. Ed.*, 2010, **49**, 9685–9688; (c) J. Stiller, E. Marqués-López, R. P. Herrera, R. Fröhlich, C. Strohmann and M. Christmann, *Org. Lett.*, 2011, **13**, 70–73; (d) M. Silvi, C. Cassani, A. Moran and P. Melchiorre, *Helv. Chim. Acta*, 2012, **95**, 1985–2006; (e) G. Talavera, E. Reyes, J. L. Vicario and L. Carrillo, *Angew. Chem., Int. Ed.*, 2012, **51**, 4104–4107; (f) B. S. Donslund, K. S. Halskov, L. A. Leth, B. M. Paz and K. A. Jørgensen, *Chem. Commun.*, 2014, **50**, 13676–13679; (g) C. Martín-Santos, C. Jarava-Barrera, S. del Pozo, A. Parra, S. Díaz-Tendero, R. Mas-Ballesté, S. Cabrera and J. Alemán, *Angew. Chem., Int. Ed.*, 2014, **53**, 8184–8189; (h) L. Naesborg, K. S. Halskov, F. Tur, S. M. N. Mønsted and K. A. Jørgensen, *Angew. Chem., Int. Ed.*, 2015, **54**, 10193–10197.

9 (a) M. Balletti, E. Marcantonio and P. Melchiorre, *Chem. Commun.*, 2022, **58**, 6072–6075. For the direct excitation of dienamines, which was limited to the use of tertiary bromomalonates as the only suitable radical precursors, see: (b) M. Silvi, E. Arceo, I. D. Jurberg, C. Cassani and P. Melchiorre, *J. Am. Chem. Soc.*, 2015, **137**, 6120–6123; (c) During the preparation of this manuscript, a photoredox/enamine dual catalysis protocol was reported detailing two entries for the remote perfluoroalkylation of  $\alpha$ -branched enals with poor reactivity but good stereocontrol, see: M. Briand, L. D. Thai, F. Bourdreux, N. Vanthuyne, X. Moreau, E. Magnier, E. Anselmi and G. Dagoussset, *Org. Lett.*, 2022, **24**, 9375–9380.

10 (a) E. Arceo, I. D. Jurberg, A. Álvarez-Fernández and P. Melchiorre, *Nat. Chem.*, 2013, **5**, 750–756; (b) G. A. Russell and K. Wang, *J. Org. Chem.*, 1991, **56**, 3475–3479; (c) D. Cantacuzène, C. Wakselman and R. Dorme, *J. Chem. Soc., Perkin Trans. 1*, 1977, 1365–1371; (d) A. Postigo, *Eur. J. Org. Chem.*, 2018, **46**, 6391–6404.

11 (a) T. Ishino and T. Oriyama, *Chem. Lett.*, 2007, **36**, 550–551; (b) H. Sato, F. Nagashima and T. Oriyama, *Chem. Lett.*, 2010, **39**, 379–381; (c) C. Ma, Z.-J. Jia, J.-X. Liu, Q.-Q. Zhou, L. Dong and Y.-C. Chen, *Angew. Chem., Int. Ed.*, 2013, **52**, 948–951.

12 (a) I. Arenas, A. Ferrali, C. Rodríguez-Escrich, F. Bravo and M. A. Pericàs, *Adv. Synth. Catal.*, 2017, **359**, 2414–2424; (b) T. Inoshita, K. Goshi, Y. Morinaga, Y. Umeda and H. Ishikawa, *Org. Lett.*, 2019, **21**, 2903–2907.

13 The EDA complex interaction could be elicited by halogen bonding between the nitrogen lone pair of the dienamine and the  $\sigma$ -hole on the iodine atom of  $R_F\text{-I}$ . Our efforts to obtain suitable crystals of the EDA aggregate, which would have provided clear insights on the nature of this interaction, had unfortunately met with failure. For a review on the importance of halogen bonding in EDA complexes involving perfluoroalkyl iodides, see: A. Postigo, *Eur. J. Org. Chem.*, 2018, 6391–6404.

14 The sense of asymmetric induction, as deduced by the absolute configuration of product **3g** based on X-ray analysis, is consonant with the dienamine reacting with an *s-cis* geometry, as depicted for intermediate **II** in Fig. 5. This conformational behaviour of dienamines formed from  $\alpha$ -phenyl enals is a consequence of 1,3-allylic strain; its effect on the stereochemical outcome of dienamine-promoted asymmetric processes has been already observed: C. Cassani and P. Melchiorre, *Org. Lett.*, 2012, **14**, 5590–5593.

15 (a) D. D. M. Wayner, J. J. Dannenberg and D. Griller, *Chem. Phys. Lett.*, 1986, **131**, 189–191; (b) C. P. Andrieux, L. Gelis, M. Medebielle, J. Pinson and J. M. Saveant, *J. Am. Chem. Soc.*, 1990, **112**, 3509–3520.

16 (a) A. Bahamonde and P. Melchiorre, *J. Am. Chem. Soc.*, 2016, **138**, 8019–8030; (b) F. Juliá, T. Constantin and D. Leonori, *Chem. Rev.*, 2022, **122**, 2292–2352.

17 (a) L. Buzzetti, G. E. M. Criszena and P. Melchiorre, *Angew. Chem., Int. Ed.*, 2019, **58**, 3730–3747; (b) M. A. Cismesia and T. P. Yoon, *Chem. Sci.*, 2015, **6**, 5426–5434.

